Colloidal Aggregation in a Nematic Liquid Crystal: Topological Arrest of Particles by a Single-Stroke Disclination Line

Takeaki Araki and Hajime Tanaka

Institute of Industrial Science, University of Tokyo, Meguro-ku, Tokyo 153-8505, Japan

We numerically study many-body interactions among colloidal particles suspended in a nematic liquid crystal, using a fluid particle dynamics method, which properly incorporates dynamical coupling among particles, nematic orientation, and flow field. Based on simulation results, we propose a new type of interparticle interaction in addition to well-known quadrupolar interaction for particles accompanying Saturn-ring defects. This interaction is mediated by the defect of the nematic phase: upon nematic ordering, a closed disclination loop binds more than two particles to form a sheetlike dynamically arrested structure. The interaction depends upon the topology of a disclination loop binding particles, which is determined by aggregation history.

Colloidal particles are usually suspended in an isotropic liquid such as water and oil. When colloidal particles are dispersed in a nematic liquid crystal, which is a liquid with long-range orientational order, the director field of a nematic solvent around particles is distorted due to surface anchoring effects of particles. This feature leads to very complex elastic interactions among them [1–9]. Thus, aggregation behavior is expected to be different from that in an isotropic liquid. This topic has recently attracted considerable attention since it may open up novel applications of colloidal suspensions [2,10,11]. It may also have a biological relevance since proteins often exist in a liquid crystalline phase [12].

Here we consider a situation where a particle accompanies a disclination line of $s = -1/2$ [13] around its equator, which is called Saturn-ring defect. This type of defect is known to be formed when small particles are dispersed in a nematic liquid crystal and directors tend to align perpendicular to the colloid surface (so-called homeotropic anchoring). A set of a particle and its Saturn-ring defect has a quadrupolar symmetry, which causes a quadrupolar interaction between the particles [1,4,5,14,15]. Furthermore, it was shown that complex many-body interaction can be predicted by a coarse-grained description of a particle-defect pair [5]. However, competition between particle surface anchoring of point symmetry and far-field director field of a different symmetry leads to a richer variety of interparticle interactions than previously thought. For example, Guzmán *et al.* [16] recently reported a defect structure which is different from the quadrupolar symmetry, in a confined geometry. Thus, many-body interactions among particles accompanying Saturn-ring defects remain elusive. In this Letter, we propose a new type of interparticle interactions mediated by a disclination line, based on the results of our numerical simulation. We also demonstrate that the selection of a defect structure depends upon aggregation history.

Since interactions between particles mediated by the elasticity of a nematic solvent intrinsically have many-body nature, it is very difficult to describe the forces acting on particles analytically [1,3–5]. Thus, numerical simulations are often employed to predict behavior of such systems [16–19]. Recently we proposed a new method for simulating the dynamics of colloidal suspension in nematic liquid crystal including nematohydrodynamic effects [20] by introducing a nematic order parameter to a "fluid particle dynamics (FPD)" method [21]. Our method enables us to simulate full dynamical coupling among particles, nematic orientational order and flow field, which are the three relevant physical variables to describe this system. To get rid of the solid-liquid boundary condition of the velocity field, which makes simulation of colloidal suspensions quite difficult, we treat solid particles as undeformable fluid particles having a higher viscosity than the solvent in FPD [21]. In our FPD method, other degrees of freedom, such as ion concentration for a charged colloidal system [22] and a concentration field for a binary mixture [23], can be introduced straightforwardly, since the flow field of the solvent is solved as a continuous field.

Here we briefly explain our numerical method. The coarse-grained variables necessary for the physical description of dynamics of colloids suspended in an anisotropic host fluid are the colloidal particle position $\{r_\alpha\}$, nematic order parameter Q_{ij} [24], and fluid velocity field v. Here index α stands for an individual particle. We express particle α using a function $\phi_\alpha(r)$ as $\phi_\alpha(r) = [\tanh\{(a - |r - r_\alpha|)/\xi\} + 1]/2$, where a and ξ are the radius and interface width of the particle, respectively [21]. For a nematic liquid crystal, we employ the following free energy functional:

$$\mathcal{F}\{Q_{ij}, \phi\} = \int dr \Big\{ f(Q_{ij}, \phi) + \frac{K_1}{2}(\partial_k Q_{ij})^2 + \frac{K_2}{2}(\partial_i Q_{ij})^2$$
$$- W\xi Q_{ij}\partial_i\phi\partial_j\phi - E_i E_j Q_{ij} \Big\}. \tag{1}$$

Here $\phi(r) = \sum_\alpha \phi_\alpha(r)$ is the concentration field representing the particle distribution. The first term of Eq. (1) is the free energy of a bulk nematic phase given by $f(Q_{ij}, \phi) = -\frac{1}{2}A(1 - 2\phi)Q_{ij}Q_{ji} - \frac{1}{3}BQ_{ij}Q_{jk}Q_{ki} + \frac{1}{4}C(Q_{ij}Q_{ji})^2$, where B and C are the positive constants. A is negative and positive above and below the transition, respectively. Note that even below the transition, the inside of particles remains negative since $A(1 - 2\phi) < 0$. The second and third terms of Eq. (1) represent the Frank elasticity: K_1 and K_2 are their elastic moduli. The fourth term is the anchoring energy of the nematic phase at the particle surface: W is the energetic cost of the anchoring per unit area. The fifth term represents a coupling between an external (electric or magnetic) field E_i and the director field.

Time evolution of Q_{ij} and $\boldsymbol{v}$ is then described by

$$\frac{DQ_{ij}}{Dt} = Q_{ik}\Omega_{kj} - \Omega_{ik}Q_{kj} + \frac{H_{ij}}{\mu_1} + \frac{\mu_2 A_{ij}}{2\mu_1} + \lambda_{ij}, \quad (2)$$

$$\rho\frac{Dv_i}{Dt} = F_i - \phi\partial_i\mu + Q_{jk}\partial_i H_{jk} + \partial_j(H_{ik}Q_{kj} - Q_{ik}H_{kj})$$
$$- \partial_i p + \partial_j\Sigma_{ij}. \quad (3)$$

Here, $\mu = \frac{\delta}{\delta\phi}\mathcal{F}$ and $H_{ij} = -\{\frac{\delta}{\delta Q_{ij}}\mathcal{F} - \frac{1}{d}\delta_{ij}\delta_{kl}\frac{\delta}{\delta Q_{kl}}\mathcal{F}\}$ are the effective chemical potential for particle concentration ϕ and the molecular force field for nematic order Q_{ij}, respectively [24]. $A_{ij} = \frac{1}{2}(\partial_i v_j + \partial_j v_i)$ and $\Omega_{ij} = \frac{1}{2} \times (\partial_i v_j - \partial_j v_i)$ are symmetric and asymmetric velocity gradient tensors. $\Sigma_{ij} = \beta_1 Q_{ij}Q_{kl}A_{kl} + (\beta_4(\phi) - \frac{\mu_2^2}{2\mu_1})A_{ij} + \frac{\beta_5 + \beta_6}{2}(Q_{ik}A_{kj} + A_{ik}Q_{kj}) - \frac{\mu_2}{2\mu_1}H_{ij}$ is a mechanical stress tensor for the flow field [25,26]. β_1, β_4, β_5, β_6, μ_1, and μ_2 are constants having a dimension of viscosity. In the spirit of FPD, the shear viscosity depends on the particle configuration as $\beta_4 = \bar{\beta}_4 + \Delta\beta_4\phi(r)$ [21]. Here $\bar{\beta}_4$ and $\bar{\beta}_4 + \Delta\beta_4$ correspond to the shear viscosities outside and inside a fluid particle, respectively. Here $\boldsymbol{F}(r) = \sum_\alpha \boldsymbol{F}_\alpha\phi_\alpha(r)/\int dr\phi_\alpha(r)$ is the force field calculated from the force directly acting on particle α, $\boldsymbol{F}_\alpha$: $\boldsymbol{F}_\alpha = -\frac{\partial}{\partial r_\alpha}\sum_\beta V(|r_\beta - r_\alpha|)$, where $V(r)$ is the direct interparticle interaction. We employed the repulsive part of the 12-6 Lennard-Jones potential as $V(r)$, whose length is set to be $2a$. λ_{ij} in Eq. (2) is the thermal fluctuation for Q_{ij}. Here we impose the thermal fluctuation only for Q_{ij} for simplicity. We assume that the density of a colloidal particle is the same as that of a host fluid; thus, the density ρ is constant. Pressure p is determined to satisfy the incompressible condition $\partial_i v_i = 0$. Time evolution of the position of particle α is described by the average fluid velocity inside the particle as $dr_\alpha/dt = \int dr\boldsymbol{v}(r)\phi_\alpha(r)/\int dr\phi_\alpha(r)$. The length, time, and force are normalized by the characteristic length $\Xi = \sqrt{K_1/A}$, characteristic rotational time $t_Q = \mu_1\Xi^2/K_1$, and elastic modulus K_1, respectively. We denote the scaled value of variable x as $\tilde{x}$.

In this Letter, we employ the following parameters: the Reynolds number $\frac{\rho K_1}{\eta\mu_1} = 0.02$, the ratio between the two Frank elasticity moduli $K_2/K_1 = 0.5$, $B/A = 25$, $C/A = 20$, and $\tilde{W} = 10$ (strong anchoring). We denote the degree of orientational order of the nematic phase as $Q_0 = \frac{B + \sqrt{B^2 + 24AC}}{6C}$. The ratios between the viscosities of the nematic phase are as follows: $\mu_1 Q_0^2/\eta = 0.65$, $-\frac{\mu_2}{2\mu_1 Q_0} = 2.0$, $\frac{(\beta_5 + \beta_6)Q_0}{2\eta} = 0.06$, and $\beta_1 Q_0^2/\eta = 0.1$, where $\eta = \bar{\beta}_4 - \frac{\mu_2^2}{2\mu_1}$ is a viscosity for usual shear flow. As an FPD parameter, the viscosity difference between the inner and outer part of the particle is set to be $(\bar{\beta}_4 + \Delta\beta_4)/\bar{\beta}_4 = 50$. We assume $\xi = \Xi$ for simplicity and set ξ to a lattice size. We solved the time development of the particle positions and the orientational field [Eq. (2)] using the explicit Euler scheme, and the flow field [Eq. (3)] by a MAC (maker and cell) method with a staggered lattice [27]. The time increment was $\Delta\tilde{t} = 0.01$.

First we study how a pair of particles (with homeotropic anchoring) interact with each other after an isotropic-to-nematic transition. Our simulations reveal two configurations under a weak external field: (a) the well-known configuration stabilized by the quadrupolar interaction and (b) a new type of (quasi-)stable configuration, where a pair of particles are bound by a "figure of eight" disclination loop. Figures 1(a) and 1(b) show the formation process of structures (a) and (b), respectively.

We initially place a pair of particles ($\tilde{a} = 6$) with the interparticle separation $\Delta\tilde{r} = 14$ in an isotropic phase of a liquid crystal. At $\tilde{t} = 0$, we quench a system to the nematic phase while applying an external field $E_z = 0.1$ perpendicularly to the line connecting the particle centers and imposing thermal orientational fluctuations $|\lambda_{ij}| = 1 \times 10^{-2}$. In the early stage, the nematic ordering is affected by the surface anchoring and the external field. As a result, formed is a transient defect configuration, which is symmetric to both the external field and particle positions [Figs. 1(a) and 1(b) ($\tilde{t} = 30$)]. This structure is quite similar to one found by Guzmán *et al.* [16] under a strong
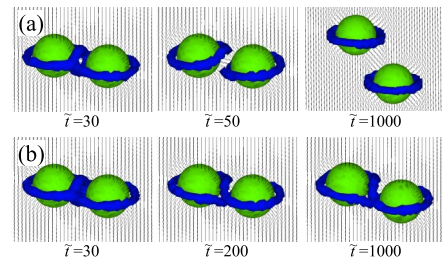

FIG. 1 (color online). Two types of defect formation processes around a pair of particles. A transient defect structure formed in the early stage ($\tilde{t} = 30$) becomes unstable and transforms into either (a) the lowest energy structure stabilized by the quadrupolar interaction or (b) a new type of (quasi-)stable configuration, in which a single disclination loop is shared by two neighboring particles.

spatial confinement between two parallel walls with ho-
meotropic anchoring [28].

In our case, this structure appears only transiently and
transforms into the lower-energy configurations [see
Fig. 1(a) ($\tilde{t} = 50$) and Fig. 1(b) ($\tilde{t} = 200$)]. The final
configurations are selected randomly by the thermal noise
λ_{ij}. When two nodes are broken in the same side of the
disclination, the two separated ring defects are formed as in
Fig. 1(a) ($\tilde{t} = 50$). As time elapses, the particles move to
form the stable quadrupolar configuration [see Fig. 1(a)
($\tilde{t} = 1000$)]. There the separation between the particles is
$\Delta r/(2a) \cong 1.4$ and the angle between the direction of the
external field and the line connecting the particle centers is
nearly 50°. This is characteristic of the quadrupolar con-
figuration reported previously [1,4,5,14,15]. On the other
hand, when nodes in the opposite side are disconnected,
only a single disclination loop having a "figure of eight"
structure remains [Fig. 1(b) ($\tilde{t} = 200$)]. The disclination
loop tends to shrink to reduce the elastic energy, but does
not cross itself due to a high energy barrier for such
topological change. We can say that the particles are
topologically arrested by a closed disclination loop. Here
the particle centers sit on a plane perpendicular to the
external field and their separation is $\Delta r/(2a) \cong 1.1$. This
defect structure has a chirality. The two types of chiral
structures can be created with an equal probability. Even
more than three particles can be bound by a single-stroke
disclination loop by the same mechanism. Since a discli-
nation loop tends to be formed on a plane perpendicular to
the director field, a sheetlike planar aggregate is formed
(see the inset of Fig. 3). We note that the interaction
depends on the interparticle separation in a nontrivial
manner due to the intrinsically nonlocal nature.

We confirmed that the stored elastic energy of configu-
ration (a) is lower than that of two isolated ones with
separated Saturn-ring defects, as shown previously [1,4].
Since there is no energy barrier between these configura-
tions, isolated particles can smoothly form configuration
(a). On the other hand, the stored elastic energy of the
"figure of eight" defect structure [Fig. 1(b)] is higher by
$\sim 150 k_B T$ than that of two isolated particles [30]. However,
once this structure is formed, it remains as it is due to a
large barrier for the topological change of the defect struc-
ture. As shown above, this structure is not selected ener-
getically but kinetically: a local minimum configuration on
the kinetic path.

Next we show the aggregation dynamics of a many-
particle system in Fig. 2. At $\tilde{t} = 0$, we quenched the system
from an isotropic phase to a nematic one without applying
any external field. Just after the quench, nematic ordering
takes place in a solvent. Reflecting nematic ordering, dis-
clination lines emerge and their length quickly decreases
with time. Since the particle motion is slow compared to
defect motion, the defects are trapped by particles in the
early stage ($\tilde{t} \lesssim 10$). In this stage, most defects are strongly
elongated and entangled complicatedly. Disclination lines,

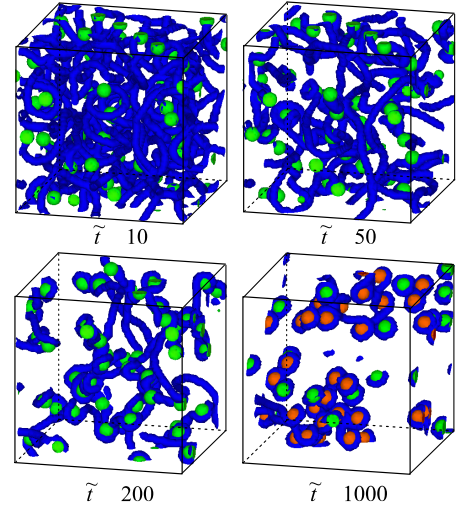

FIG. 2 (color online). The aggregation process of particles
immersed in a liquid crystal. A simulated box (64^3) includes
50 particles of $\tilde{a} = 3.5$ ($\Phi = 3.43\%$). Particles bound by dis-
clination lines are drawn as red ones.

which are shared by particles far apart, shrink to lower the
elastic energy: This induces hydrodynamic motion of par-
ticles (see below). Particles sharing a defect can interact
even when there exist other particles between them. This
means that the interaction mediated by a disclination line
depends upon the topology of the disclination line: this
leads to an intrinsically nonadditive nature, which is
stronger than for the case of localized defects. Shrinking
of defects while keeping their topology results in the for-
mation of clusters of particles bound by disclination lines.
In this way, the topologically arrested metastable structures
are kinetically selected as a result of the orientational
ordering from an isotropic state, despite that they are in a
high energy state.

The elastic force (or tension) acting on a disclination
line arises not only from the line itself, but also from a
viscous drag force to particles trapped. When the elongated
defect line cannot support the tension, it is disconnected in
the process of the shortening and isolated Saturn-ring
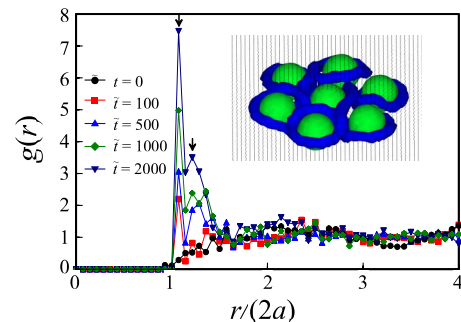defects are formed around the individual particles. Such

FIG. 3 (color online). Time development of $g(r)$. The inset
shows a sheetlike planar aggregated structure composed of seven
particles bound by a single-stroke defect loop.

particles then interact with each other via the quadrupolar interaction and form configuration (a) in Fig. 1(a) ($\tilde{t}=$ 1000). We note that a population of such isolated Saturn-ring defects is higher for a more dilute dispersion. This is because the stronger tension acts on disclination lines due to a larger average interparticle distance, which leads to more frequent disconnection of disclination lines. For example, a rather few topologically arrested structures exist in the late stage for the volume fraction of $\Phi = 3.43\%$ [see red particles in Fig. 2 ($\tilde{t} = 1000$)].

The formation process of the two types of defect structures can be clearly seen in the time development of the radial distribution function of particles, which is calculated as $g(r) = \sum_{\alpha\beta}\delta(r - |\boldsymbol{r}_\alpha - \boldsymbol{r}_\beta|)/(4\pi r^2 \delta r \Phi)$. For example, Fig. 3 shows the temporal change of $g(r)$ for a rather dense colloidal dispersion, which contains 125 particles (its volume fraction is 8.56%). $g(r)$ has two growing peaks around $r/(2a) \cong 1.1$ and 1.4, which correspond to configuration (a) and (b) in Fig. 1, respectively. This double-peak feature reflects the peculiar aggregation process of particles suspended in a nematic liquid crystal, which is driven by the two types of attractive interactions.

Here we stress that to properly treat the effect of hydrodynamic drag force and the resulting tension-induced disconnection of a disclination, solving the director field of a nematic solvent with hydrodynamics is essential. In a nematic liquid crystal without particles, an inhomogeneous director field with defects can be relaxed to a homogeneous one only via the local rotation of the director. Thus, the defect motion accompanies rather localized flow, which is induced by flow-orientation coupling effect [25]. When it contains particles, however, disclination lines are pinned by particles due to the topological constraint. In this case, particles are transported hydrodynamically to reduce the stored elastic energy. Thus, we may say that the hydrodynamic flow is induced not only by shrinking disclination lines alone, but also by the entire deformed director field around the particles: particle-mediated delocalization of nematohydrodynamic interactions.

In sum, we proposed a new type of a defect structure, which binds more than two particles. The interaction depends upon the topology of a disclination line binding particles, which is further affected by aggregation history. Such a defect structure has not been reported experimentally. One of the possible reasons for this is that particles accompanying Saturn rings are very small for usual conditions [e.g., $2a \lesssim 600$ nm for $W > 10^{-4}$ N/m [4]; see also [30]]. Although direct observation of the defect structure may not be so easy, we hope that its existence will be experimentally confirmed (directly or indirectly) in the near future.

[1] R. W. Ruhwandl and E. M. Terentjev, Phys. Rev. E **55**, 2958 (1997).
[2] P. Poulin *et al.*, Science **275**, 1770 (1997).
[3] T. C. Lubensky *et al.*, Phys. Rev. E **57**, 610 (1998).
[4] H. Stark, Phys. Rep. **351**, 387 (2001).
[5] B. I. Lev *et al.*, Phys. Rev. E **65**, 021709 (2002).
[6] P. Poulin and D. A. Weitz, Phys. Rev. E **57**, 626 (1998).
[7] J. C. Loudet, P. Barois, and P. Poulin, Nature (London) **407**, 611 (2000).
[8] M. Yada, J. Yamamoto, and H. Yokoyama, Phys. Rev. Lett. **92**, 185501 (2004).
[9] I. I. Smalyukh *et al.*, Phys. Rev. Lett. **95**, 157801 (2005).
[10] S. P. Meeker *et al.*, Phys. Rev. E **61**, R6083 (2000); V. J. Anderson *et al.*, Eur. Phys. J. E **4**, 11 (2001).
[11] J. Yamamoto and H. Tanaka, Nature (London) **409**, 321 (2001).
[12] S. V. Shiyanovskii *et al.*, Phys. Rev. E **71**, 020702(R) (2005).
[13] Throughout the Letter, a disclination line means this type.
[14] J. C. Loudet *et al.*, Langmuir **20**, 11 336 (2004).
[15] O. Mondain-Monval *et al.*, Eur. Phys. J. B **12**, 167 (1999).
[16] O. Guzmán *et al.*, Phys. Rev. Lett. **91**, 235507 (2003); O. Guzmán, N. L. Abbott, and J. J. de Pablo, J. Polym. Sci., B Polym. Phys. **43**, 1033 (2005).
[17] M. Tasinkevych *et al.*, Eur. Phys. J. E **9**, 341 (2002).
[18] J. Fukuda *et al.*, Phys. Rev. E **69**, 041706 (2004).
[19] R. Yamamoto, Phys. Rev. Lett. **87**, 075502 (2001); R. Yamamoto, Y. Nakayama, and K. Kim, J. Phys. Condens. Matter **16**, S1945 (2004).
[20] T. Araki and H. Tanaka, J. Phys. Condens. Matter **18**, L193 (2006).
[21] H. Tanaka and T. Araki, Phys. Rev. Lett. **85**, 1338 (2000); Chem. Eng. Sci. **61**, 2108 (2006).
[22] H. Kodama *et al.*, J. Phys. Condens. Matter **16**, L115 (2004).
[23] T. Araki and H. Tanaka, Phys. Rev. E **73**, 061506 (2006).
[24] P. G. de Gennes and J. Prost, *The Physics of Liquid Crystals* (Clarendon, Oxford, 1993).
[25] G. Tóth, C. Denniston, and J. M. Yeomans, Phys. Rev. Lett. **88**, 105504 (2002); D. Svenšek and S. Žumer, Phys. Rev. E **66**, 021712 (2002).
[26] T. Araki and H. Tanaka, Phys. Rev. Lett. **93**, 015702 (2004).
[27] F. H. Harlow and J. E. Welch, Phys. Fluids **8**, 2182 (1965).
[28] This configuration has two disclination nodes, each of which has four-arms defects. Since line defects having the charge ($-1/2$) interact with each other repulsively, a four-arms defect structure in the configuration has a higher elastic energy than two separated defects [29]. Thus, it should be separated into two disclinations if the constraint from the walls is relaxed. We consider that the configuration reported by Guzmán *et al.* is characteristic of the confined geometry with a mirror symmetry.
[29] I. Chuang *et al.*, Phys. Rev. E **47**, 3343 (1993).
[30] We consider a system, in which the particles, whose diameter is $2a = 70$–120 nm, are suspended in a nematic solvent, whose elastic modulus is $K_1 = 0.5$ pN and correlation length $\Xi = 10$ nm. The anchoring strength is $W = 5 \times 10^{-4}$ N/m.